*Progress In Electromagnetics Research Letters, Vol. 47, 61–70, 2014*

# Analysis of Excitation Pulsed Signal Propagation for Atom Probe Tomography System

**Blaise Ravelo[1, *] and Francois Vurpillot[2]**

**Abstract**—The purpose of this paper is on the behavioral modelling of surge voltage pulses used in Atom Probe Tomography. After brief description of the atom probe functioning principle, we examine the excitation electrical pulse signal integrity along the electric pulser (E-pulser) feeding line modelling with respect to the IEC1733/04 standard. This feeding electric line is ended by cylindrical via ground to control the ion emission. By using the transmission line (TL) ultra-broadband RLCG model, the propagating pulsed signals degradation is predicted. The signal propagation was analysed in both frequency and time domains by taking into account the substrate dispersion. The wideband frequency behaviours of the surge signal along the feeding line were examined from DC-to-2 GHz. In addition, by considering pulse surge signals with pulse-width and rise-/fall-time parameters ($T_1 = 9$ ns, $t_{r1} = t_{f1} = 1.6$ ns) and ($T_2 = 30$ ns, $t_{r2} = 4$ ns/$t_{f2} = 18$ ns), the transient responses from 5 cm-to-20 cm length TL are characterized. It was shown that the excitation pulse was significantly distorted. It was emphasized that the operated signal delay varies from 0.3 ns-to-1.5 ns in function of the via capacitor value. The time-dependent radiated $E$-field on the performance of the atom probe system which enables to characterize the nature of tested materials (ions or atoms) is discussed. The presented analysis approach is particularly useful for E-pulser integrated in measurement scientific instruments as Atom Probe Tomography time of flight optimisation, a nano-analysing technique that uses ultra-sharp high vacuum pulse to induce controlled erosion of samples. In this application, the excitation voltage pulse integrity during the propagation is required in order to improve the measurement instrument performances.

## 1. INTRODUCTION

With the tremendous applications and growth of the need for high speed operating data in modern electronic structures, electrical interconnect effect becomes drastically significant [1, 2]. This degradation effect increases with the signal propagation speed through the design interconnect distribution. One of the most usual cases can be found during the complex printed circuit boards (PCBs) design cycle. Due to the interconnect lines unmatching, several electromagnetic (EM) and electrical phenomena need to be predicted during the characterization of high speed signals as electrical fast transient (EFT) and surge voltages/currents behaviors. Owing to such an effect, various numerical and analytical modelling methods of interconnect lines for high speed signal sharing were developed [3–6]. Those easy and fast computational methods are subsequently integrated by electronic design engineers in their circuit models in order to predict the signal integrity (SI) especially when the operating frequency is higher [2–6]. So far, most conducted investigations were intended to predict the behavior of standard RF/digital signals. However, the SI analysis is still an open challenge when the operating signal presents arbitrary shapes with high intensity. For this reason, the SI investigation addressed in this paper is focused on pulsed arbitrary shape signals with some ns time-width. The particular example to be treated in this study

*Received 24 April 2014, Accepted 18 June 2014, Scheduled 28 July 2014*
* Corresponding author: Blaise Ravelo (blaise.ravelo@yahoo.fr).
[1] IRSEEM EA 4353, ESIGELEC, Av. Galilée, Saint Etienne du Rouvray 76801, France. [2] GPM UMR 6634 CNRS, Univ. Rouen, Av. de l'Université, Saint Etienne du Rouvray 76801, France.

relies on the analysis of typically EFT signals presenting kV range amplitude for the complex structures as Atom Probe scientific instruments [7].

### 1.1. Atom Probe Tomography Description

The Atom Probe Tomography understudy was invented in the GPM laboratory of the University of Rouen [8–12]. This scientific instrument is used for the microscopic materials characterization. The electrical circuit diagram enabling the EM characterization of the Atom Probe Tomography system understudy is sketched in Figure 1. This technique is regularly used by physicists for the atom scale material samples mass spectroscopy. This atom probe instrument is essentially composed of electric pulser (E-pulser) circuit exhibiting surge voltage $U(t)$. As functioning principle, the excitation pulses are applied to a counter electrode in front of the sample, a sharp needle [8]. The surge electric pulses induce the time control ionisation of surface atoms. The produced ions are projected on a position sensitive detector placed at a distance $L$ from the sample. The time of flight of ions, i.e., the duration of the flight of ions between the pulse start time and the impact stop time is used to establish time-of-flight mass spectrometry. More details on the overall functioning and especially all physical aspects about the atom probe microscopy technique can be found in the literature [13, 14]. Different applications were developed more recently notably for the microscopic material characterization [15] and for investigating atomic force microscope tips and interfacial phenomena [16].

It should be noted that the atom probe system operates in Ultra High Vacuum (UHV), and the sample undergoes a DC voltage and is exposed under cryogenic temperature. The accuracy of the time of flight measurement is related to the measurement of the stop time (lower than 50 ps on the detector), and the spread of time and energy is induced by the applied electric pulse. The amplitude of voltage pulses required to generate the ionisation of surface atoms is expressed in the kV range with width in the nanosecond range. In addition, a pulse repetition rate of several kHz is required. We employ in our application conventional pulses generated with high power MOSFET transistor [17]. This kind of device can produce multi-kilovolts square waveform voltage pulses with a few nanosecond rise time. This pulse is reshaped in order to reach a few nanoseconds width with a passive RC discharge circuit. To improve the accuracy of the measurement system, a new generation of pulse generator producing sub-nanosecond E-pulses with rise and trailing edges lower than 100 ps is currently under development based on the concept introduced in [18, 19]. In electrical point of view, the E-pulser circuit can be practically assumed as a transmission line (TL) terminated by via hole as depicted in Figure 2. A surge signal with very low rise-/fall-time and width is necessary for the improvement of the atom probe performances. Of course, it is fundamentally crucial to the experimenter physicists using the tomographic atom probe to analyse and to preserve the integrity of the excitation voltage signal at the extremity of the line.

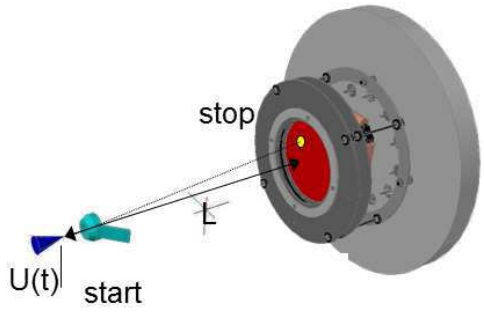


**Figure 1.** Termination of the atomic probe instrument invented in GPM laboratory [7].

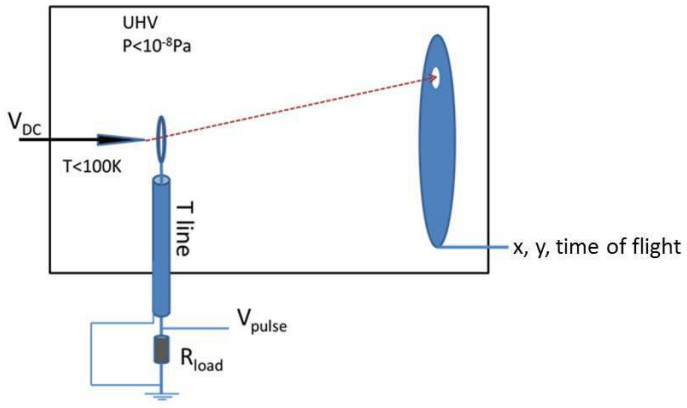


**Figure 2.** Illustrative schematic diagram of the Tomographic Atom Probe including the feeding line understudy [12].

### 1.2. Outline of the Paper

Remember that the last part of feeding line of the atom probe must be compatible with UHV atmosphere and must support the high power generated by the system. In other words, a special care must be taken to develop a propagation line delivering non-perturbed signal to the sample. Therefore, the present study is mainly focused on the electrical modelling of this probing system circuit termination by using the interconnect line RLCG model. First, much attention was paid to the creation of the pulse signal according to the technique depicted in Figure 2. It is worth noting that the response of surge transient pulse signal through the microstrip line designed with respect to the IEC 1733/04 standard [20] termination by considering a capacitive via will be investigated.

For the better understanding, this paper is organized in three main sections. Section 2 is dedicated to the analytical approach based on the electrical circuit broadband model of the interconnect line implemented to control the atom probe time of flight. Section 3 is focused on the analysis of the application results. Finally, Section 4 draws the conclusion.

## 2. BEHAVIORAL MODEL OF THE E-PULSER SYSTEM

The electrical equivalent circuit of the atom probe excitation system understudy is mainly composed of TL driven by a voltage source herein denoted $v_{in}$ with internal impedance $Z_s$ ended by output load impedance $Z_L$ as proposed in [2, 3]. The input and output currents delivered by the source and propagating across the load are denoted as $i_{in}$ and $i_{out}$, respectively. To determine those electrical parameters, we will first consider the dispersive properties of the substrate used in the E-pulser feeding microstrip line as illustrated in Figure 3.

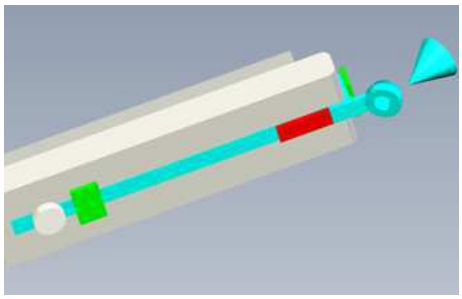

**Figure 3.** Illustrative design of the Atom Probe Tomography feeding microstrip line termination [12].

Then, we determine the TL characteristic elements (propagation constant $\gamma(j\omega)$ and characteristic impedance $Z_c(j\omega)$) in broadband frequency according to the bandwidth of the surge signal under considerations. The extracted parameters are integrated in the system transfer function in order to generate the E-pulser output voltage $V_{out}(j\omega)$ and the operating currents $I_{in}(j\omega)$ and $I_{out}(j\omega)$ via analytical behavioral modelling. In the last step, the corresponding transient signals are extracted via IFFT.

### 2.1. Frequency-Dependent Model of the E-Pulser Substrate

In addition to the application of the behavioral model, in the present study, we will challenge the difficulty encountered regularly by SI engineers on the integration of material and TL structures frequency dependent parameters. To do this, the frequency dependent permittivity of the substrate material which is governed by relaxation behavior is approximated by the Debye frequency dispersion model expressed as:

$$\varepsilon_{eff}(j\omega) = \varepsilon_\infty + (\varepsilon_s - \varepsilon_\infty)/(1 + j\omega\tau) + \sigma/(j\omega\varepsilon_0), \tag{1}$$

with $j$ is the complex number. During the numerical computation, the Debye parameters are set as $\varepsilon_s = 4$ is the static permittivity, $\varepsilon_\infty = 3$ is the high-frequency limit permittivity, $\tau = 1\,\text{ns}$ is the relaxation time; and $\sigma = 1.25 \times 10^{-6}\,\mu\text{S}\cdot\text{m}^{-1}$ is the ohmic equivalent conductivity. Actually, there may be several Debye terms describing frequency dependence of the dielectric as FR4.

### 2.2. Analytical Model of the E-Pulser

There are different configurations of microstrip lines used regularly for microwave interconnections [20–22]. The structures understudy are assumed either microstrip (standard IEC1733/04) or strip lines (standard IEC1734/04) [20] physically characterized by metallization width $w$ and thickness $t$ printed on the substrate having height $h$ and dielectric constant $\varepsilon_r$. For the case of strip line structures, the substrate thickness is designated by the parameter $b$. According to the operating frequency ranges under consideration, we will use the simplified expressions of TL characteristic impedances. Based on the feeding line implementation technology, the characteristic impedance main formulas in function of the effective relative permittivity $\varepsilon_{eff}(\omega)$ are respectively defined as:

$$Z_c(\omega) = \frac{87}{1.41 + \sqrt{\varepsilon_{eff}(\omega)}} \ln\left(\frac{5.98h}{0.8w + t}\right), \tag{2}$$

for classical microstrip lines,

$$Z_c(\omega) = \frac{60}{\sqrt{\varepsilon_{eff}(\omega)}} \ln\left(\frac{5.98h}{0.8w + t}\right), \tag{3}$$

for embedded ones in the medium with effective relative permittivity $\varepsilon_{eff}$ and finally:

$$Z_c(\omega) = \frac{60}{\varepsilon_{eff}(\omega)} \ln\left(\frac{4b}{0.67\pi w\,(0.8 + t/w)}\right), \tag{4}$$

for the strip lines. Moreover, according to the TL theory, the broadband (including low- and high-frequency bands) per-unit length parameters ($R_u$, $L_u$, $C_u$, $G_u$) can be extracted with the following formulas:

$$R_u(\omega) = \begin{cases} 1/(t \cdot w \cdot \sigma) \text{ in DC} \\ \sqrt{\mu_0 \cdot \omega/(2\sigma \cdot w^2)} \text{ in HF} \end{cases}, \tag{5}$$

$$L_{u\,\text{in nH/m}}(\omega) \approx 3.386 Z_c(\omega)\sqrt{\varepsilon_{eff}(\omega)}, \tag{6}$$

$$C_{u(5\%)\,\text{in pF/m}}(\omega) \approx \begin{cases} \dfrac{55.512\varepsilon_{eff}(\omega)}{\ln(8h/w + w/(4h))} \text{ for microstrip lines} \\ \dfrac{35.433\varepsilon_{eff}(\omega)}{\ln(1 + 2h/w)} \text{ for strip lines} \end{cases}, \tag{7}$$

$$G_u(\omega) = C_u(\omega)\left[\omega \tan(\delta(\omega)) + \sigma/(\varepsilon_{eff}(\omega)\varepsilon_0)\right]. \tag{8}$$

The corresponding propagation constant is computed via the basic definition:

$$\gamma(j\omega) = \sqrt{[R_u(j\omega) + jL_u(j\omega)] \cdot [G_u(j\omega) + jC_u(j\omega)]}. \tag{9}$$

### 2.3. Analytical Behavioral Model of the E-Pulser

It can be demonstrated from the TL theory that the Fourier transform of output voltage and current through the loaded line are respectively expressed as:

$$\frac{V_{out}(j\omega)}{V_{in}(j\omega)} = \frac{Z_c(j\omega)}{Z_S(j\omega) + Z_c(j\omega)} \left[\frac{e^{-\gamma(j\omega)d} + r_L(j\omega)e^{-\gamma(j\omega)d}}{1 - r_S(j\omega)r_L(j\omega)e^{-2\gamma(j\omega)d}}\right], \tag{10}$$

$$I_{out}(j\omega) = \frac{V_{in}(j\omega)}{Z_S(j\omega) + Z_c(j\omega)} \left[\frac{e^{-\gamma(j\omega)d} - r_L(j\omega)e^{-\gamma(j\omega)d}}{1 - r_S(j\omega)r_L(j\omega)e^{-2\gamma(j\omega)d}}\right], \tag{11}$$

with the input and output reflection coefficients are given by:

$$r_{S,L}(j\omega) = \frac{Z_{S,L}(j\omega) - Z_c(j\omega)}{Z_{S,L}(j\omega) + Z_c(j\omega)}. \tag{12}$$

In the remainder part of the paper, expressions (10) and (11) will be implemented into Matlab program for computing numerically the spectrum of the E-pulser frequency responses. Afterwards, $v_{out}(t)$ and $i_{out}(t)$ will be plotted via the IFFT operation.

## 3. E-PULSER SIGNAL RESPONSES ANALYSES

As aforementioned, the behavioral broadband model will be handled to generate the E-pulser feeding line circuit responses by taking into account the material substrate dispersion effect as formulated earlier in (1). After calculation of the broadband RLCG-model, we extracted then the $Z$-matrices and $S$-parameters and also the transfer function generating the results presented in the following subsection.

We will use on a microstrip line driven by a pulser voltage source is defined with reference impedance $Z_s = 50\,\Omega$ and ended by via capacitor with parameter switched between $C_L = 1\,\text{pF}$ and $10\,\text{pF}$. This access line was printed on FR4-substrate with physical width $w = 1\,\text{mm}$ and thickness $h = 1.6\,\text{mm}$ etched on Cu-metallization having $35\,\mu\text{m}$ thickness. One points out that the present tomographic atom probe feeding line modelling is added with the parametric SI analysis versus line physical length $d$ which is varied from 5 cm to 20 cm.

### 3.1. Frequency Results Analysis

The frequency spectrums of the arbitrary signals $v_1$ and $v_2$ under consideration are respectively plotted in Figure 4(a) and Figure 4(b). Independent from amplitude, this preliminary step enables to explore the relation between the rise-/fall-times of the pulses with the propagating frequency components of the signals through the access line. From there, we can analyse, in the frequency domain, the convolution between the TL transfer function of the E-pulser system for atom probe tomography [12]. This frequency plot suggests how the broadband model bandwidth should be implemented to get an accurate response.

We emphasize that according to standard EN 60512-25-7 [20], we have to avoid the resonance effect due to the TL critical length in the frequency band of interest. Similar to the microstrip line network modelling approach introduced in [6], we determined the broadband RLCG model, then we extracted the frequency dependent $Z$-matrix and the transfer function. From the input impedance of the whole

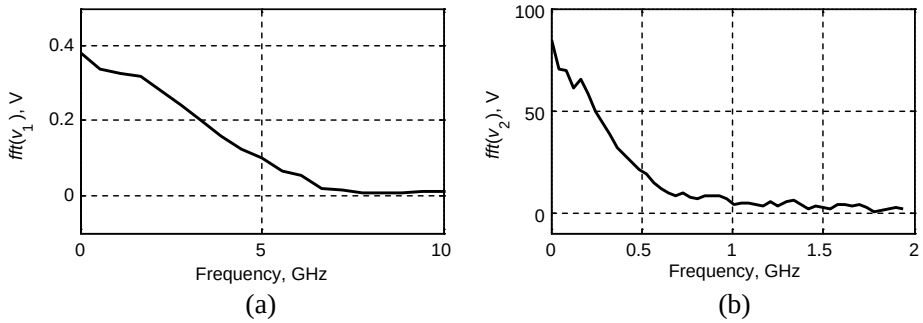


**Figure 4.** Spectrums of test signals (a) $V_1$ and (b) $V_2$.

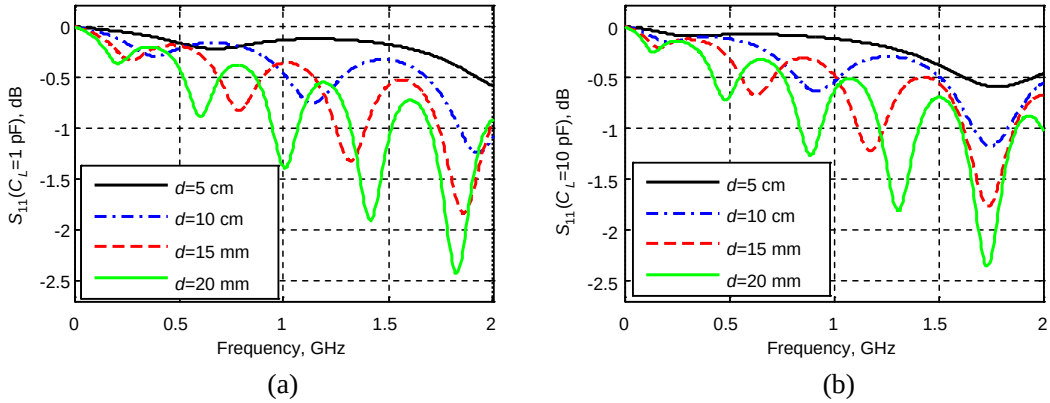


**Figure 5.** Reflection parameters of the TL system understudy vs $d$.

circuit, we obtain the reflection parameters presented in Figure 5. As forecasted in theory, it can be seen that the TL is not well matched especially at very low frequencies and when the access line length is shorter. The capacitor value slightly influences the resonance peaks of the access lines; however, the reflection level does not change significantly from DC to 2 GHz.

### 3.2. Transient Results Analysis

In order to investigate the integrity of the surge pulse voltages $v_1$ and $v_2$ whose frequency spectrums are addressed in Figure 4, transient analyses were carried out. By exciting the atom probe structure with the first sample pulse having 5 V amplitude, we generate the transient responses displayed in Figure 6(a) for $C_L = 1$ pF and Figure 6(b) for $C_L = 10$ pF. It is worth noting that the signal propagation delay increases from about 0.3 ns to 1.5 ns when changing the feeding length $d$ from 5 cm to 20 cm. More importantly, with low values of $C_L$, the pulse voltage $v_{out}$ intensity is slightly increased. Then, due to the resonance effect, attenuated ripples are observed after the tailing edge of the outputs $v_{out}$.

The transient responses of the second sample of excitation pulse assumed as high intensity pulse having 1.5 kV amplitude are highlighted in Figure 7. This transient result illustrates that the leading edge of the pulse generates signal propagation delay from about 0.7 ns to 3.5 ns when increasing $d$ from 15 cm to 55 cm. The trailing edge which presents a fall-time of about 18 ns undergoes the same delay. In order to improve the fidelity of those pulse signals, different types of well-matched optimized RLC load can be implanted. It is interesting to point out that the output voltage amplitudes is slightly amplified compared to the inputs due to the multiple reflections at the terminal of the lines.

### 3.3. Propagating Transient Currents along the E-Pulser

As aforementioned earlier, the mathematical handling of expression (11) enables to plot the transient current propagating along the atom probe E-pulser feeding line structure. After numerical computation, we obtain the results displayed in Figure 8 and Figure 9 with the feeding line input and output currents

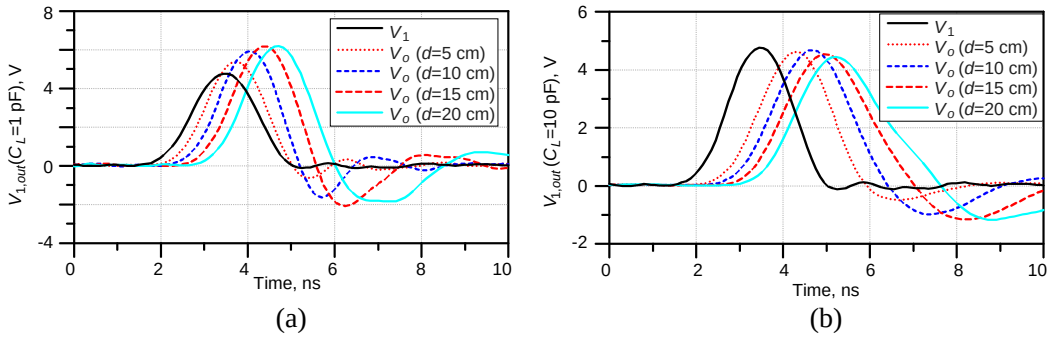


**Figure 6.** Transient responses of the system excited by $V_1$ vs $d$.

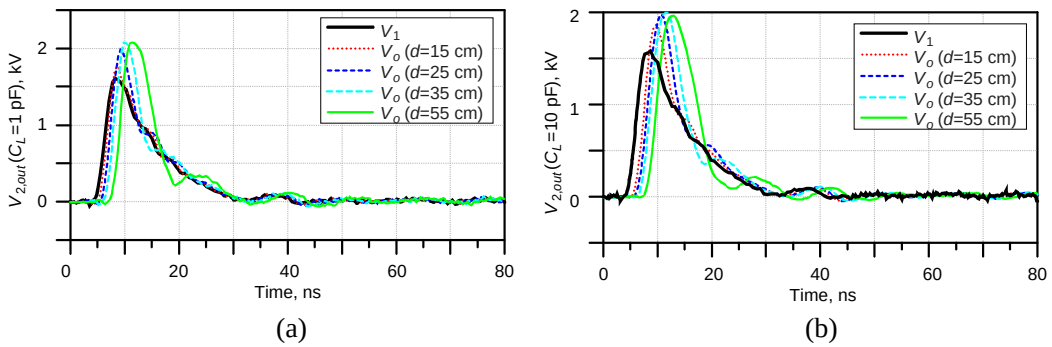


**Figure 7.** Transient responses of the system excited by $V_2$ vs $d$.

respectively for the loads $C_L = 1\,\text{pF}$ and $C_L = 10\,\text{pF}$. As expected in circuit theory, the output transient current behavior behaves as the time derivative of the corresponding voltage. Moreover, the output current propagation delay is increased with the feeding line length.

It is clear that the output currents $i_{out}$ are slightly attenuated compared to $i_{in}$. Furthermore, it is noteworthy that the attenuation is rather proportional to the feeding line length. This finding illustrates the E-pulser feeding line loss effect on the atom probe time of flight. In addition, input and output transient currents exhibited by the structure are displayed in Figure 10 and Figure 11 when exciting the structure with $v_2$. In this case, we can underline that the signal-to-noise ratio is increased for the case of the output current plotted in bottom of Figure 10.

Similar to the previous case, as highlighted by Figure 11, the signal delay and attenuation are stronger when the load capacity is increased. Substantially, we can see that the signals are slightly distorted. In inference of this parametric study, contrary to the output voltages, the output currents

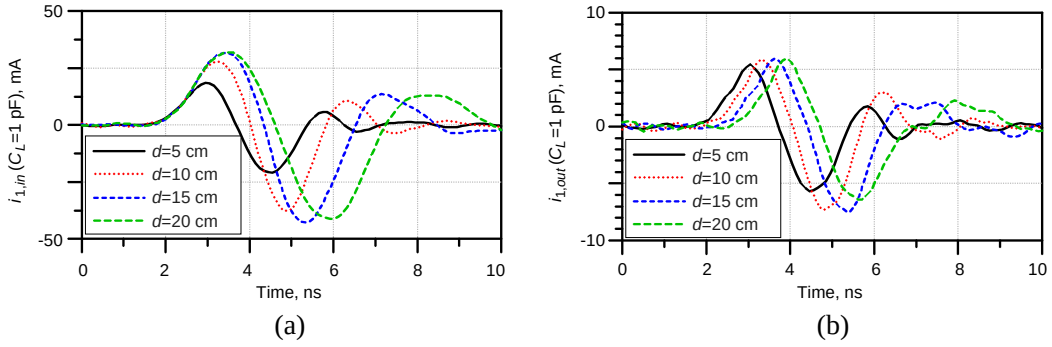


**Figure 8.** Transient currents for the input excitation $v_1$ and $C_L = 1\,\text{pF}$.

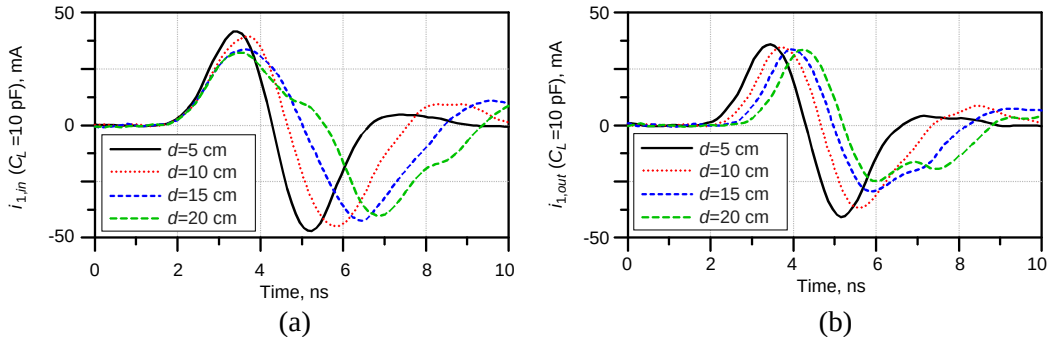


**Figure 9.** Transient currents for the input excitation $v_1$ and $C_L = 10\,\text{pF}$.

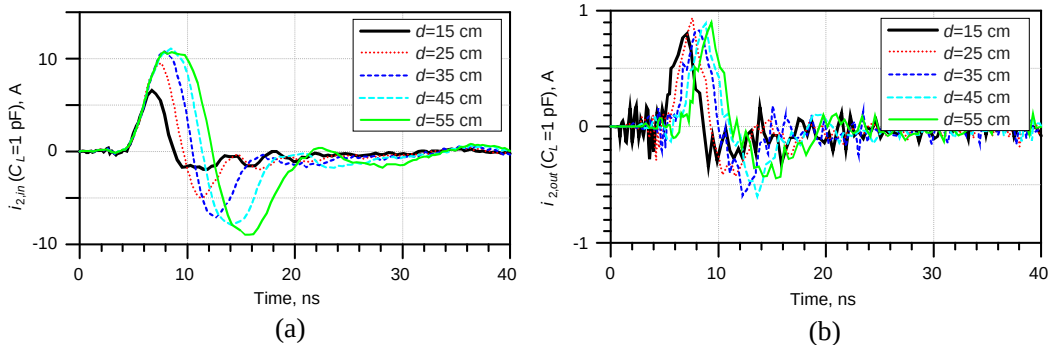


**Figure 10.** Transient currents corresponding to the input excitation $v_2$ for $C_L = 1\,\text{pF}$.

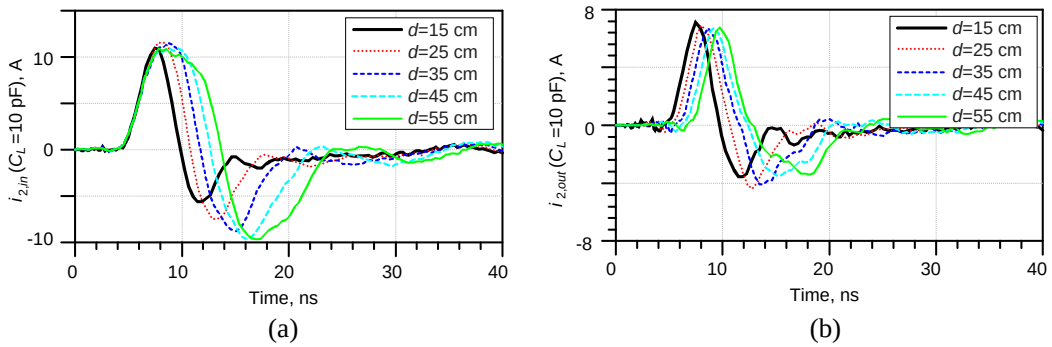


**Figure 11.** Transient currents corresponding to the input excitation $v_2$ for $C_L = 10\,\text{pF}$.

are attenuated. We underline that the computation time of the present modelling method implemented into Matlab run with PC equipped by windows 7 having Intel® Core™ i5-2467M CPU @ 1.6 GHz 4 Go RAM was of about some microseconds.

### 3.4. Discussion on the Atom Probe Performance

According to the physical analysis introduced in [12, 13], the ratio between the mass $m$ and quantity $n$ of atom particles operated with the system introduced in Figure 1 is equated by:

$$m/n = 2 \cdot F^2 \cdot e \cdot E \cdot \tau / L, \tag{13}$$

where $e$ is the electron charge, $\tau$ the propagation time, $E$ the amplitude of the electric field evaporating the tested material samples, and $F$ a physical factor. This relation explains that the inaccuracy on the electric field amplitude and also the pulse propagation time affects significantly the precision of the mass spectrum. With the feeding line parameters chosen in this section, the average values of transient electrical field radiated along the axis of the cylindrical via was about $E_1 = 2\,\text{kV/m}$ and $E_2 = 1.2\,\text{MV/m}$ respectively for $v_1$ ($d = 20\,\text{cm}$, $C_L = 10\,\text{pF}$) and $v_2$ ($d = 55\,\text{cm}$, $C_L = 10\,\text{pF}$). The system accuracy can be minimized in function of the feeding line parameters. This study is helpful for the GPM laboratory physicists to evaluate and optimize the E-pulser according to the sample of material to be tested.

## 4. CONCLUSION

A computational modelling of the fast pulsed signal propagation on microstrip lines under IEC1733/04 standard [20] ended by capacitive via was investigated. Analytical approaches based on the TL theory associated to the broadband per unit length parameters extraction were considered in order to generate the output responses for various shapes of excitation signals.

We proposed a preliminary study on the Atom Probe Tomography time of flight improvement dedicated to the mass spectroscopy. Parametric analyses by varying the TL dimensions with length swept from 5 cm-to-20 cm for the short test signal and 15 cm-to-55 cm for the long test signal were forwarded. Input signals having ns rise-/fall-times and tens nanoseconds width from practical tests were injected in the structure. It was pointed out that the transient output voltages were delayed of about some nanoseconds with non-neglected ringing effects. More importantly, the first analyses on the transient E-pulse atom probe along via holes showed that considerable signal time-width was also occurred. This time parameter is susceptible to influence the quality of mass spectroscopy. Compared to the existing methods, the presented model is beneficial in term of simplicity, flexibility to the shape of the E-pulser feeding line and also the computation speed.

The present analysis is interesting for implementing UHV atom probe tomography for the mass spectroscopy application in function of the transmission line parameters. This enables to reduce the mass inaccuracy and also the energy losses with the increase of pulse width.

In the future, the surge signal modelling developed in this work can be extended for the conducted EMC and electrostatic discharge investigations on high density PCBs interconnect distribution networks under arbitrary shape signal perturbations.

## ACKNOWLEDGMENT

Acknowledgement is made to the Upper Normandy Region for the PULSAT project support of this research work through the FEDER fund.

## REFERENCES

1. Deutsch, A., G. V. Kopcsay, P. Restle, G. Katopis, W. D. Becker, H. Smith, P. W. Coteus, C. W. Surovic, B. J. Rubin, R. P. Dunne, T. Gallo, K. A. Jenkins, L. M. Terman, R. H. Dennard, G. A. Sai-Halasz, and D. R. Knebel, "When are transmission-line effects important for on-chip interconnections?," *IEEE Trans. Microwave Theory and Techniques*, Vol. 45, 1836–1846, Oct. 1997.
2. Eudes, T., B. Ravelo, T. Lacrevaz, and B. Fléchet, "Distributed model of two-level asymmetrical PCB interconnect tree," *Proc. of 2013 International Symposium on Electromagnetic Compatibility (EMC Europe)*, 132–137, Brugge, Belgium, Sep. 2–6, 2013.
3. Ravelo, B., "Delay modelling of high-speed distributed interconnect for the signal integrity prediction," *Eur. Phys. J. Appl. Phys.*, Vol. 57 31002-1–31002-8, Feb. 2012.
4. Buckwalter, J. F., "Predicting microwave digital signal integrity," *IEEE Trans. Advanced Packaging*, Vol. 32, No. 2, 280–289, May 2009.
5. Zhang, G.-H., M. Xia, and X.-M. Jiang, "Transient analysis of wire structures using time domain integral equation method with exact matrix elements," *Progress In Electromagnetics Research*, Vol. 92, 281–298, 2009.
6. Ravelo, B., "Behavioral model of symmetrical multi-level T-tree interconnects," *Progress In Electromagnetics Research B*, Vol. 41, 23–50, 2012.
7. Müller, E. W., J. A. Panitz, and S. B. McLane, "The atom probe field ion microscope," *Review of Scientific Instruments*, Vol. 39, No. 1, 83–88, 1968.
8. Blavette, D., A. Bostel, J. M. Sarrau, B. Deconihout, and A. Menand, "An atom-probe for three dimensional tomography," *Nature*, Vol. 363, 432–435, 1993.
9. Gault, B., F. Vurpillot, A. Vella, M. Gilbert, A. Menand, D. Blavette, and B. Deconihout, "Design of a femtosecond laser assisted tomographic atom probe," *Review of Scientific Instruments*, Vol. 77, No. 4, 043705, 2006.
10. Kelly, T. F. and M. K. Miller, "Atom probe tomography," *Review of Scientific Instruments*, Vol. 78, No. 3, 031101, 2007.
11. Menand, A. and D. Blavette, "Sonde atomique tridimensionnelle," P902, 1–7, Techniques de l'Ingénieur, Jul. 1995 (in French).
12. Vurpillot, F. and A. Bostel, "Tomographic atomic probe comprising a high voltage electric pulse electro-optical generator," Patent No. 057721, 2010.
13. Gault, B., M. P. Moody, J. M. Cairney, and S. P. Ringer, "Atom probe microscopy," *Springer Series in Materials Science*, Vol. 160, 29–68, 2012.
14. Kelly, T. F., T. T. Gribb, J. D. Olson, R. L. Martens, J. D. Shepard, S. A. Wiener, T. C. Kunicki, R. M. Ulfig, D. R. Lenz, E. M. Strennen, E. Oltman, J. H. Bunton, and D. R. Strait, "First data from a commercial local electrode atom probe (LEAP)," *Microscopy and Microanalysis*, Vol. 10, 373–383, 2004.
15. Miller, M. K., "Atom probe tomography and field ion microscopy: Ion-beam techniques," *Characterization of Materials*, 2nd Edition, May 2012, Doi: 10.1002/0471266965.com145.
16. Tourek, C. J., "Application of atom probe tomography to the investigation of atomic force microscope tips and interfacial phenomena," Ph.D. Thesis, Iowa State University, USA, 2012.
17. www.belke.com.
18. Kohler, S., V. Couderc, R. P. O'connor, D. Arnaud-Cormos, and P. Lévêque, "A versatile high voltage nano- and sub-nanosecond pulse generator," *IEEE Trans. Dielectrics and Electrical Insulation*, Vol. 20, No. 4, 1201–1208, Aug. 2013.

19. Yuan, J., W. Xie, H. Liu, J. Liu, H. Li, X. Wang, and W. Jiang, "High-power semi-insulating GaAs photoconductive semiconductor switch employing extrinsic photoconductivity," *IEEE Trans. Plasma Sci.*, Vol. 37, No. 10, 1959–1963, Oct. 2009.
20. European Standard, "Connector for electronic equipment — Tests measurements — Part 25-7: Test 25g — Impedance, reflection coefficient and voltage standing wave ratio (VSWR)," NF EN 60512-25-7, Jun. 2005.
21. Blood, Jr., W. R., *ECL System Design Handbook*, 45 & 48, Motorola Semiconductor Products, Inc., Phoenix, AZ, 1988.
22. Buchanan, J. E., *BiCMOS/CMOS Systems Design,* 109, McGraw-Hill, New York, 1991.